Neurofilament Subunit NF-H Modulates Axonal Diameter by Selectively Slowing Neurofilament Transport

Joseph R. Marszalek,* Toni L. Williamson,§ Michael K. Lee,‖ Zuoshang Xu,‡‡ Paul N. Hoffman,¶ Mark W. Becher,‖ Thomas O. Crawford, and Don W. Cleveland*‡§**

*Division of Cellular and Molecular Medicine, ‡Departments of Medicine and Neuroscience, and §Ludwig Institute for Cancer Research, University of California at San Diego, La Jolla, California 92093; Departments of ‖Pathology, ¶Ophthalmology, and **Neurology, The Johns Hopkins University School of Medicine, Baltimore, Maryland 21205; and ‡‡Worcester Foundation for Biomedical Research, Shrewsbury, Massachusetts 01545

Abstract. To examine the mechanism through which neurofilaments regulate the caliber of myelinated axons and to test how aberrant accumulations of neurofilaments cause motor neuron disease, mice have been constructed that express wild-type mouse NF-H up to 4.5 times the normal level. Small increases in NF-H expression lead to increased total neurofilament content and larger myelinated axons, whereas larger increases in NF-H decrease total neurofilament content and strongly inhibit radial growth. Increasing NF-H expression selectively slows neurofilament transport into and along axons, resulting in severe perikaryal accumulation of neurofilaments and proximal axonal swellings in motor neurons. Unlike the situation in transgenic mice expressing modest levels of human NF-H (Cote, F., J.F. Collard, and J.P. Julien. 1993. *Cell.* 73:35–46), even 4.5 times the normal level of wild-type mouse NF-H does not result in any overt phenotype or enhanced motor neuron degeneration or loss. Rather, motor neurons are extraordinarily tolerant of wild-type murine NF-H, whereas wild-type human NF-H, which differs from the mouse homolog at >160 residue positions, mediates motor neuron disease in mice by acting as an aberrant, mutant subunit.

SINCE the initial visualization of neurofilaments by silver staining in the early nineteenth century, mounting evidence has pointed to their importance in specifying axonal diameter (caliber) (Friede and Samorajski, 1970; Hoffman et al., 1987; Cleveland et al., 1991; Lee and Cleveland, 1994). The increase in axonal diameter, which initiates concomitantly with myelination and continues at a slow rate throughout adulthood, is important for normal functioning of the nervous system, since caliber is a principal determinant of the conduction velocity at which nerve impulses are propagated along the axon (Gasser and Grundfest, 1939; Arbuthnott et al., 1980; Sakaguchi et al., 1993). Assembled as obligate heteropolymers (Ching and Liem, 1993; Lee et al., 1993) of three polypeptide subunits, NF-L (68 kD), NF-M (95 kD), and NF-H (115 kD), neurofilaments are the most abundant cytoskeletal components in large myelinated axons. The importance of neurofilaments in specifying normal axonal caliber has recently been proven unequivocally by analysis of a recessive mutation (*quv*) in a Japanese quail that lacks neurofilaments as the result of a premature translation terminator in the NF-L gene (Ohara et al., 1993). Radial growth fails completely in these animals (Yamasaki et al., 1992; Ohara et al., 1993), with a consequent reduction in axonal conduction velocity and generalized quivering (Sakaguchi et al., 1993). Nearly total inhibition of neurofilament transport into axons by expression of a NF-H–β-galactosidase fusion protein in transgenic mice has also been shown to result in similar inhibition of radial growth of large myelinated axons (Eyer and Peterson, 1994).

Although it is clear that neurofilaments are important for specifying axonal diameter, the mechanism through which neurofilaments mediate increase in axonal size remains unsettled. The linear correlation between neurofilament number and axonal cross-sectional area initially suggested that the axon expanded or contracted to maintain a constant density of neurofilaments (Friede and Samorajski, 1970; Hoffman et al., 1987). However, analysis of transgenic mice that express elevated levels of wild-type NF-L reveals that despite a two- to threefold increase in number of neurofilaments, the axonal diameter actually decreases slightly (Monteiro et al., 1990; Xu et al., 1993). Thus, while neurofilaments are required for normal radial growth of myelinated axons, determination of axonal diameter is specified by other factors in addition to simple neurofilament number. Since the long, highly phosphorylated tail domains of NF-H and, to a lesser extent, NF-M

Address all correspondence to Don W. Cleveland, Ludwig Institute for Cancer Research, University of California, San Diego, 9500 Gilman Drive, La Jolla, CA 92093. Tel.: (619) 534-7811. Fax: (619) 534-7659. e-mail: dcleveland@ucsd.edu

have been implicated as a regulator of neurofilament spacing in axons (de Waegh et al., 1992; Hsieh et al., 1994; Nixon et al., 1994), one reasonable postulate is that in mice expressing high levels of NF-L, dilution of these tail domains results in inhibition of proper radial growth.

Correlative evidence suggests that NF-H has a special modulatory role in neurofilament-dependent radial growth of axons. Although the expression level of NF-L and NF-M mRNA increases more modestly, the increase in the level of NF-H mRNA is most pronounced during the rapid radial growth phase (0–4 wk postnatal) (Schlaepfer and Bruce, 1990). Indirect evidence for an essential role of NF-H in radial growth has emerged from doubling NF-M content through expression of an epitope-tagged NF-M transgene. This yields a 50% reduction in axonal NF-H and strongly inhibits radial growth, despite a constant level of NF-L (Wong et al., 1995). Furthermore, it is now well established that the tail domains of NF-M and NF-H project from the "core" filament both in vitro (Hirokawa et al., 1984; Troncoso et al., 1990) and in mature axons (Hirokawa et al., 1984). Phosphorylation of these tail domains is strongly correlated with radial growth. For example, in the *Trembler* mouse a primary defect in myelination decreases phosphorylation of NF-H, increases neurofilament density, and inhibits normal radial growth of axons (de Waegh et al., 1992). Similarly, unmyelinated initial segments have dephosphorylated NF-H, higher filament packing density (Hsieh et al., 1994; Nixon et al., 1994), and much smaller diameters than the adjacent myelinated segments. Moreover, slowing of slow axonal transport during early postnatal development correlates with the increases in NF-H expression, prompting the suggestion that NF-H modulates the rate of slow axonal transport (Willard and Simon, 1983).

In addition to the normal role of neurofilaments in radial growth of myelinated axons, the observations that abnormal accumulations of neurofilaments are an early common pathological hallmark in patients with motor neuron disease (Carpenter, 1968; Chou and Fakadej, 1971; Hirano et al., 1984*a,b*; for review see Hirano, 1991) have led to the hypothesis that abnormalities in neurofilament organization may be involved in the pathogenesis of human motor neuron disease, including amyotrophic lateral sclerosis (ALS).[1] Furthermore, it is now clear that neurofilament abnormalities can cause motor neuron disease in some transgenic mouse models. Specifically, high levels of wild-type neurofilament subunit expression, either murine NF-L (Xu et al., 1993) or human NF-H (Cote et al., 1993), in transgenic mice lead to perikaryal and axonal accumulation of neurofilaments accompanied by motor neuron dysfunction and neurogenic atrophy of skeletal muscle. Furthermore, expression of a modest level of a mutant NF-L subunit leads to both cytoskeletal abnormalities and selective death of large spinal motor neurons (Lee et al., 1994).

We have now directly tested the role of NF-H in neurofilament-dependent radial growth of large myelinated axons by producing a series of transgenic mice that synthesize NF-H at varying levels. Increasing wild-type murine NF-H content in neurons selectively retards neurofilament transport while it accelerates transport of other cytoskeletal proteins. Modest increases in NF-H mildly enhance radial growth, but higher levels severely retard growth. Even 4.5 times as much murine NF-H does not result in overt phenotype or motor neuron dysfunction despite perikarya extraordinarily distended with aggregated neurofilaments and inhibition of radial growth. Since this contrasts with progressive neuronopathy reported in mice expressing lower levels of human NF-H (Cote et al., 1993; Collard et al., 1995), human NF-H must cause disease in mice by acting as a mutant subunit.

Materials And Methods

Production and Screening of Transgenic Mice

The 23-kb SalI fragment from a mouse NF-H cosmid (Cos 3A1; Julien et al., 1988) containing the entire mouse NF-H coding region and the 15 kb of 5′ flanking region (see Fig. 1 *A*) were purified by electroelution after agarose gel electrophoresis. The DNA was microinjected into pronuclei of one-cell mouse embryos obtained by mating C57B6 × C3 F1 females with C57B6 males. Mouse pups were analyzed for the presence of the NF-H transgene by DNA blotting of mouse tail DNA as described (Monteiro et al., 1990; Xu et al., 1993). Tail DNAs were digested with EcoRV, separated on 0.8% agarose gels, and transferred to GeneScreen Plus membranes (New England Biolabs, Beverly, MA). The membrane was incubated with 1×10^6 cpm/ml of probe prepared by random primer extension using [α-^{32}P]dATP and a 1.4-kb EcoRV/AatII fragment from NF-H gene containing the sequences encoding some of the KSP multiphosphorylation repeats and part of the NF-H 3′ flanking region. A 5-kb transgene-specific fragment was diagnostic for transgenic animals with greater than one transgene copy integrated in tandem.

Analysis of Neurofilament RNA Levels in Nervous Tissues

Spinal cords and dorsal root ganglia were removed from NF-H transgenic and wild-type mice and immediately frozen and stored at −80°C. Total cellular RNA was purified using TRIzol reagent (GIBCO BRL, Gaithersburg, MD) and the method provided by manufacturer. RNA for 1-yr-old animals was extracted by homogenization of tissue in 4 M guanidinium thiocyanate, 25 μM sodium citrate, pH 7, 0.1 M 2-metcaptoethanol, and 0.5% Sarkosyl. An equal volume of acidic phenol was added, and the aqueous phase was collected after centrifugation. RNA was then precipitated with an equal volume of isopropanol and collected by centrifugation. RNA was further purified by resuspension in 4 M lithium chloride and subsequent centrifugation. The RNA was again suspended, and then precipitated with an equal volume of isopropanol. The pellet was rinsed with 75% ethanol and resuspended in 0.3% SDS. RNA concentration was determined by determining the absorbance at 260 nm.

2.5 μg (4-wk-old animals) or 2 μg (1-yr-old animals) of total RNA was fractionated on a 1% agarose gel containing 1.85% formaldehyde and, transferred to GeneScreen Plus II. The filters were baked for 2 h at 80°C, prehybridized for 1 h in 0.5 M sodium phosphate, pH 7.2, 1 mM EDTA, 7% SDS, and 1% bovine albumin, and RNAs encoding neurofilament subunits were detected by hybridization with random primed [α-^{32}P]dATP labeled nucleotide probe. Filters were then washed in 30 mM Tris, pH 7.4, and 300 mM NaCl, for 20 min at room temperature, followed by two washes (30 min each at 60°C) in 3 mM Tris, pH 7.4, 30 mM NaCl, and 0.5% SDS. RNA bands corresponding to different neurofilament subunits were visualized by autoradiography using x-ray film (XAR; Eastman-Kodak Co., Rochester, NY) and quantified by phosphorimaging (Molecular Dynamics, Sunnyvale, CA).

SDS-PAGE and Detection of Neurofilament Proteins by Immunoblotting

Sciatic nerves and spinal cords were homogenized (with a polytron homogenizer) in a buffer containing 25 mM sodium phosphate, pH 7.2, 5 mM EDTA, pH 8, and 1% SDS. The homogenates were boiled for 5 min and clarified by centrifugation at 16,000 *g* for 5 min, and supernatants were transferred to new tubes. Protein concentration was determined using the

1. *Abbreviations used in this paper*: ALS, amyotrophic lateral sclerosis; DRG, dorsal root ganglia.

bicinchoninic acid assay kit (BCA; Pierce Chemical Co., Rockford, IL). Protein extracts, as well as known amounts of neurofilament standards, were separated by SDS-PAGE using gels containing 6 or 7.5% polyacrylamide. Proteins separated by SDS-PAGE were transferred to nitrocellulose (Lopata and Cleveland, 1987). The NF-H subunit was identified using an affinity-purified rabbit polyclonal antibody (Xu et al., 1993), followed by ^{125}I-conjugated protein A. mAbs to moderately phosphorylated NF-H (RMO217 [Lee et al., 1987]), NF-M (Boehringer Mannheim Biochemicals, Indianapolis, IN), or NF-L (Sigma Chemical Co., St. Louis, MO) were used to identify each subunit, followed by rabbit anti–mouse IgG (Sigma Chemical Co.) and ^{125}I-conjugated protein A. The neuron-specific β_{III}-tubulin isotype was visualized using mAb TuJ1 (Lee et al., 1990) and processed in the same manner as the other mAbs. Immunoreactive bands were visualized by autoradiography using Kodak XAR film. Quantification was performed by phosphorimaging (Molecular Dynamics) using known amounts of purified mouse spinal cord neurofilaments as standards.

Tissue Preparation and Morphological Analysis

Transgenic and littermate control animals were anesthetized by intraperitoneal injection of (0.02 ml/g) Avertin, and one or both sciatic nerves, as well as a 0.5-cm segment of tail, were removed for biochemical analyses. Mouse tissues were then fixed by intracardial perfusion with 4% paraformaldehyde and 2.5% glutaraldehyde in 0.1 M sodium phosphate, pH 7.6. The paraformaldehyde/glutaraldehyde-fixed tissues were postfixed in the same fixative for 24 h at 4°C followed by 2% osmium tetroxide in 0.1 M phosphate buffer, dehydrated in alcohols, and embedded in Epon-Araldite resin. For light microscopy, 1-μm sections were stained with toluidine blue. Thin-sections for EM were stained with uranyl acetate and lead citrate.

Morphometric Analysis

To determine the diameters of myelinated axons, L5 ventral roots were embedded in Epon, 1-μm sections were cut and stained with toluidine blue, and sections were viewed under ×100 magnification. The images were digitized and converted to a 512 × 512 pixel video display using a video camera and frame-grabber video board. All myelinated axons were identified, and areas were determined by a morphometric software program (Bioquant MegX; R & M Biometrics, Inc., Nashville, TN). The entire nerve was measured using contiguous nonoverlapping fields with center-of-gravity exclusion to avoid double counting or size bias in the counts. Light level and optimal threshold on a 256 grey-scale were determined for each field independently. Cross-sectional area of each axon was measured and converted to a diameter of a circle of equivalent area.

Analysis of Filament Spacing: Nearest Neighbor Analysis

To measure nearest neighbor distances between neurofilaments, cross-sections of axons >3.0 μm in diameter were photographed at a magnification of 20,000 and enlarged an additional 4.25-fold by printing. Neurofilaments were identified in these end on views as dots of ~10 nm in diameter. Positions of neurofilaments were marked by puncturing the print with a pushpin. By laying the final prints on a light box, neurofilament positions could easily be imaged using a CCD camera and digitized using image analysis software (Bioquant; R & M Biometrics, Inc.), and nearest neighbor distances were calculated for each filament.

Axonal Transport Analysis

The velocity of axonally transported neurofilaments was determined in 8-wk-old transgenic and nontransgenic littermates. To metabolically label newly synthesized neurofilaments in motor axons, 300 μCi of [^{35}S]methionine was injected into the ventral horn of the lumbar spinal cord. For sensory axons, 100 μCi of [^{35}S]methionine was injected into the L5 dorsal root ganglia (DRG). 7 or 14 d after the injection, the L5 roots or DRG and ~3 cm of sciatic nerve were removed and cut into 3-mm segments. Each segment was homogenized in a buffer containing (25 mM sodium phosphate, pH 7.0, 150 mM NaCl, 1 mM EDTA, 0.9 M sucrose, 1% Triton X-100, and 2 mM PMSF) and centrifuged at 12,000 *g* for 20 min. Essentially all of the neurofilament proteins (NF-L, NF-M, and NF-H), along with cold insoluble tubulin and actin, were recovered in the pellet fraction. The entire pellet (resolubilized in 2% SDS-containing gel sample buffer) and the soluble proteins were separated by SDS-PAGE. The distribution of [^{35}S]methionine-labeled proteins was visualized by fluorography. The radioactivity associated with each of the neurofilament subunits was determined by phosphorimaging.

Results

Transgene Copy Number–dependent Increase in NF-H RNA Levels in NF-H Transgenic Mice

To examine the consequence of overexpressing wild-type murine NF-H, pronuclear microinjection of a 23-kb fragment containing the complete mouse NF-H gene (Fig. 1 *A*) was used to produce transgenic mice. 14 founders were identified using DNA blotting of mouse tail DNA (Fig. 1 *B*), 10 of which produced progeny that carried the transgene. Transgene copy number was determined by phosphorimaging analysis of duplicate blots probed for the NF-H transgene or the endogenous NF-L gene, the latter of which was used to normalize for DNA loading (Fig. 1 *B*). Five lines of mice that carry between three and 35 additional copies of the NF-H gene were selected for further analysis (NF-Hcos 35, 61, 62, 65, and 75).

To determine the level of NF-H mRNA accumulation in each transgenic line, RNA was prepared from spinal cord, DRG, and cortex of 4-wk-old animals. RNA blot analysis of spinal cord RNA showed an NF-H gene dosage-

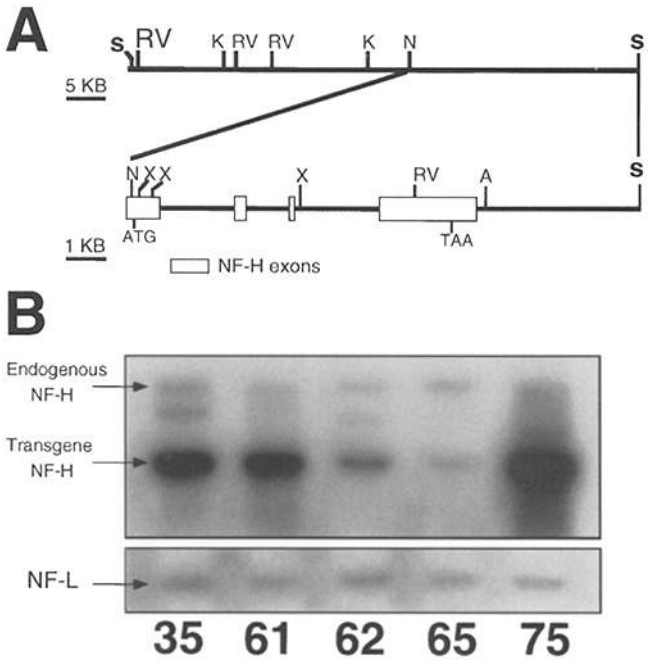

Figure 1. Lines of mice containing a transgene encoding wild-type murine NF-H. (*A*) Schematic drawing of a 23-kb SalI/SalI NF-Hcos transgene. Lower portion displays a blowup of the NF-H coding region. *S*, SalI; *RV*, EcoRV; *K*, KpnI; *N*, NotI; *X*, XhoI; *A*, AatII. (*B*) Detection of multiple transgene inserts in six lines determined by blotting genomic DNAs after digestion with EcoRV and probing with the 1.4-kb EcoRV/AatII fragment extending 3′ from the EcoRV site in exon 4. Head to tail copies of the transgene are predicted to yield a 5-kb transgene fragment; the endogenous NF-H fragment is >23 kb. (*Bottom*) To provide an internal control for DNA loading, the blot was reprobed to reveal the 3-kb endogenous NF-L gene fragment.

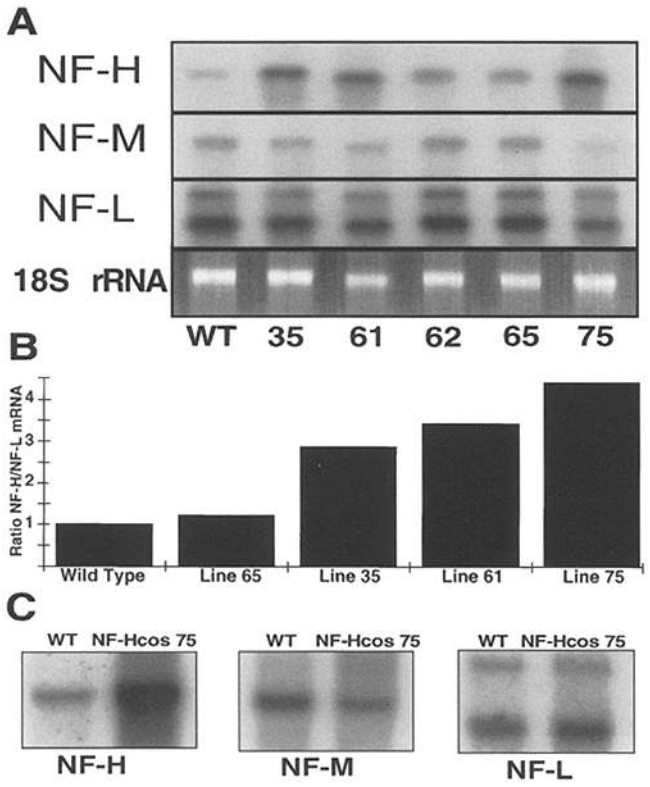

Figure 2. Increased NF-H mRNA levels in multiple transgenic lines. (*A*) RNA blots of ~2.5 μg of total RNA extracted from spinal cord of 4-wk-old mice from different transgenic lines probed for NF-L, NF-M, and NF-H RNAs. Bottom row displays the 18S rRNA region of an ethidium stained gel to verify equivalent RNA loadings. (*B*) Quantitation of the relative levels of NF-H and NF-L RNAs in the five transgenic lines. (*C*) RNA blots (probed for NF-H, NF-M, and NF-L) of spinal cord RNA from 1-yr-old transgenic line 75 or normal mice.

dependent increase in the amount of NF-H message in the different transgenic lines (Fig. 2 *A*), relative to NF-L mRNAs (Fig. 2, *A* and *B*) or 18S rRNA (Fig. 2 *A*). Similar increases in NF-H RNA levels were observed in both DRG and in cortex of NF-H transgenic mice. Phosphorimaging revealed between 1.2- and 4.5-fold increases in NF-H RNA levels relative to NF-L mRNA in the five NF-H transgenic lines (Fig. 2 *B*), and these levels remained elevated throughout life (e.g., with greater than four times the normal level in 2-yr-old heterozygotes of line 75 [Fig. 2 *C*], the highest expressing line). An unexpected finding (confirmed by phosphorimaging) was that increasing NF-H expression led to a diminution (up to twofold in 2-yr-old animals from line 75) of endogenous NF-M mRNAs (Fig. 2 *A*). Within nervous tissue, NF-H immunoreactivity is restricted to neurons (not shown), as it is in the wild-type mice. Collectively, these results show that the 23-kb NF-H transgene drives copy number–dependent increases in NF-H expression that reproduce the tissue and cellular specificity of endogenous NF-H gene expression.

Increase in NF-H Expression Leads to Reduction in Sciatic Nerve Neurofilament Content and Perikaryal Neurofilament Accumulations

To determine if the higher NF-H mRNA levels lead to increased accumulation of NF-H protein in axons, the levels of neurofilament subunits in 9-wk-old transgenic sciatic nerve extracts were analyzed by quantitative immunoblotting (Fig. 3 *A*). This revealed that in the transgenic mice with the smallest increases in NF-H RNA level (lines 65 and 62), modest (~70%) increases in NF-H subunit levels were accompanied by increases in both NF-L and NF-M levels, yielding ~25% increase in the total molar NF subunit content (Fig. 3, *A* and *B*). Despite three- to 4.5-fold higher levels of NF-H RNA levels in transgenic lines 35,

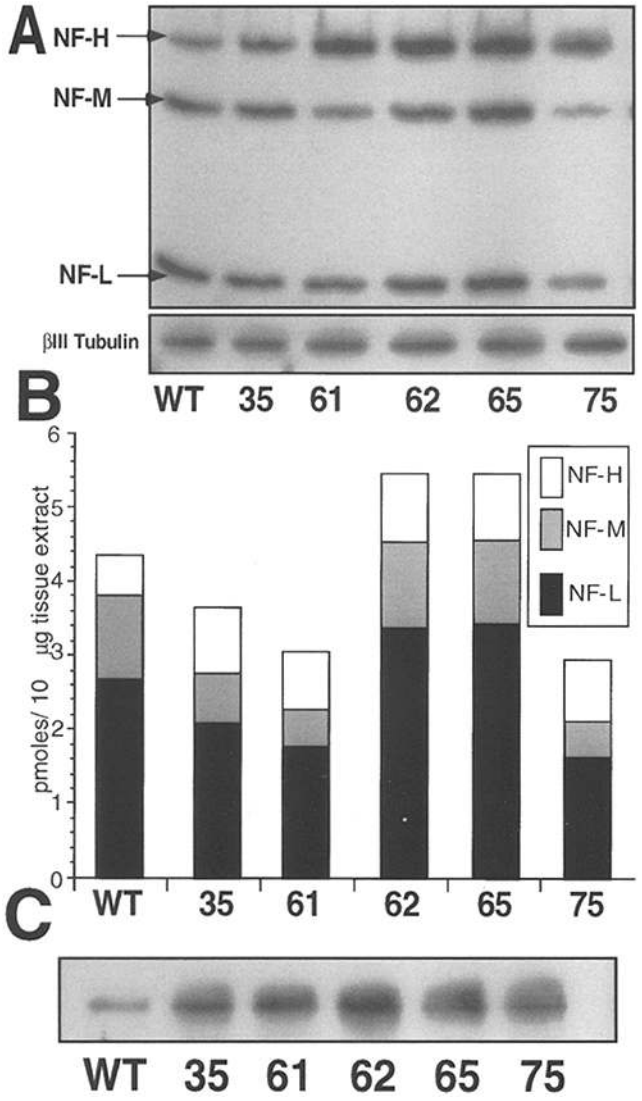

Figure 3. Immunoblotting and quantitation of neurofilament subunits in sciatic nerve of the various NF-H transgenic lines. (*A*) Immunoblot of 5 μg of total sciatic nerve protein extract from 9-wk-old animals. The three subunits were identified with a polyclonal antibody to NF-H (Xu et al., 1993), or mAbs to NF-M (Boehringer Mannheim Biochemicals) or NF-L (Sigma Chemical Co.). (*B*) Relative levels of each neurofilament subunit (in pmol per 10 μg of protein) determined by phosphorimaging of sciatic nerve immunoblots of 9-wk-old transgenic and wild-type animals (measurements are averages from three animals for each group). (*C*) Immunoblot of sciatic nerve extracts from 4-wk-old transgenic animals with an antibody (RMO217-p++) recognizing phosphorylated epitopes on NF-H (Lee et al., 1987).

61, and 75, the accumulated levels of NF-H protein in the sciatic nerve were increased only by 50–70% (denoted by the unfilled portions in Fig. 3 *B*) over the nontransgenic control. Furthermore, there were clear decreases in molar levels of both NF-L (20–40%) and NF-M (40–60%) proteins in the sciatic nerve (Fig. 3 *B*). Even with the modest increase in NF-H protein level in the sciatic nerves of line 75 with the highest NF-H RNA levels, the total molar NF content in the sciatic nerve decreased by ~30% at 9 wk (Fig. 3 *B*). Although the accumulated NF-H protein levels do not directly correlate with the NF-H mRNA levels, comparison of the molar percentage of NF-H in the sciatic nerve does increase as NF-H mRNA levels increase (Figs. 2 *B* and 3, *A* and *B*). Examination of protein levels in 4-wk-old mice yielded similar results (not shown). The amount of partially or fully phosphorylated NF-H (using mAb RMO 217; Lee et al., 1987) in the axons of all the transgenic mouse lines increased roughly in proportion to the increase in NF-H (Fig. 3 *D*). This indicates that the additional NF-H in the axons is phosphorylated to approximately the same extent as in wild-type mice. Thus, reduction of axonal caliber cannot be accounted for by a decreased phosphorylation of axonal NF-H. Metabolic labeling of isolated DRG and spinal cord did not show any obvious differences in the synthesis of NF-L subunits comparing any of the transgenic lines and wild-type mice. The discrepancy between the levels of RNA (Fig. 2 *A*) and axonal polypeptide levels (Fig. 3) must be due to differences in posttranslational processing of NF subunits.

To determine if an increase in NF-H expression also affects the accumulated levels of other axonal cytoskeletal components, the level of the neuron-specific β_{III}-tubulin isotype (Lee et al., 1990) was examined in sciatic nerves. Quantitative immunoblot analyses using the TuJ1 anti–β_{III}-tubulin antibody (Lee et al., 1990) showed that increase in NF-H expression did not have significant effects on the axonal level of neuron-specific β_{III}-tubulin (Fig. 3 *A*).

Light and electron microscopy was used to determine if changes in wild-type murine NF-H expression altered morphology of spinal and sensory neurons (as has been reported for transgenic mice expressing human NF-H to a level two to threefold above the mouse NF-H [Cote et al., 1993]). NF-H transgenic line 65, which has the smallest increase in NF-H RNA (Fig. 2), contained motor (Fig. 4 *B*) and sensory neurons (Fig. 4 *F*) indistinguishable from the neurons in normal mice (Fig. 4, *A* and *E*). However, further increases in the expression of NF-H (in lines 61 and 75) led to increasingly more severe axonal and perikaryal swellings in both spinal cord (Fig. 4, *C* and *D*) and DRG neurons (Fig. 4, *G* and *H*). The lightly stained hyaline inclusions in these swellings were confirmed to be bundles of NFs by transmission EM (data not shown). These results indicate that the increase in NF-H synthesis leads to NF-H dosage-dependent increases in perikaryal accumulation of neurofilaments and a diminution of axonal neurofilament content.

Changes in Sciatic Nerve Neurofilament Content Correlate with Changes in Caliber of Large Myelinated Axons

Since neurofilaments are a principal determinant of axonal caliber, we examined how the changes in neurofilament content in sciatic nerve were reflected in changes in axonal caliber of large myelinated axons. Light microscopic inspection of the L5 ventral (Fig. 5, *A–D*) and dorsal roots (Fig. 5, *E–H*) revealed that the large myelinated axons from NF-H transgenic lines expressing the highest levels of NF-H RNA were qualitatively smaller in caliber than those of wild-type mice (compare Fig. 5, *D–H* with *A* and *E*).

To quantify the caliber changes associated with increased NF-H expression, cross-sectional areas of every axon within each ventral root were measured in 4-wk, 9-wk, and 1-yr-old animals (Fig. 6, *A–C*). Each area was then converted to a diameter corresponding to a circle of equivalent area. As expected, nontransgenic animals showed a bimodal distribution of diameters representing the small (neurofilament-deficient) and large (neurofilament-rich) myelinated axons. In the three NF-H transgenic lines expressing the highest levels of NF-H RNA (lines 35, 65, and 75; data not shown for line 35), the increases in NF-H expression lead to a significant inhibition of radial growth of large myelinated axons at all ages (Fig. 6), consistent with the overall decrease in the axonal NF content in these mice. In the older animals, the small diameter axons (<2.5 μm) remain unchanged in number or size distribution. However, in line 65, which has the smallest increase in NF-H expression (Fig. 2), there was a modest but reproducible stimulation of radial growth of myelinated axons (Fig. 6).

Overall, these results show that a modest increase in NF-H (less than twofold) leads to increased accumulations of neurofilaments in axons accompanied by slightly increased radial growth of large myelinated axons. Larger increases in NF-H (greater than threefold) result in perikaryal and proximal axonal accumulations of neurofilaments (Fig. 4, *C*, *D*, *G*, and *H*) accompanied by a significant inhibition of radial growth (Figs. 4, *C*, *D*, *G*, and *H* and 5, *C*, *D*, *G*, and *H*).

Nearest Neighbor Spacing between Neurofilaments Is Unaffected by Increase in Axonal NF-H and the Concomitant Reduction in NF-M

To examine whether an increased proportion of NF-H and the corresponding reduction in axonal NF-M affects nearest neighbor spacing between neurofilaments, the distribution of filaments in cross-sections of ventral roots was compared from the highest expressing NF-H transgenic line (NFHcos 75) and from nontransgenic control animals. This revealed that the nearest neighbor packing of filaments was indistinguishable in transgenic and control animals (Fig. 7).

Increase in NF-H Expression Slows Axonal Neurofilament Transport

Reduction in axonal transport rates of neurofilaments with the increase in NF-H expression during development (Willard and Simon, 1983) supports a role of NF-H in modulating the rate of neurofilament transport. Such slowing of neurofilament transport has been proposed as a possible mechanism by which increases in axonal neurofilament content and accompanying radial axonal growth occur after myelination (Hoffman et al., 1983, 1984).

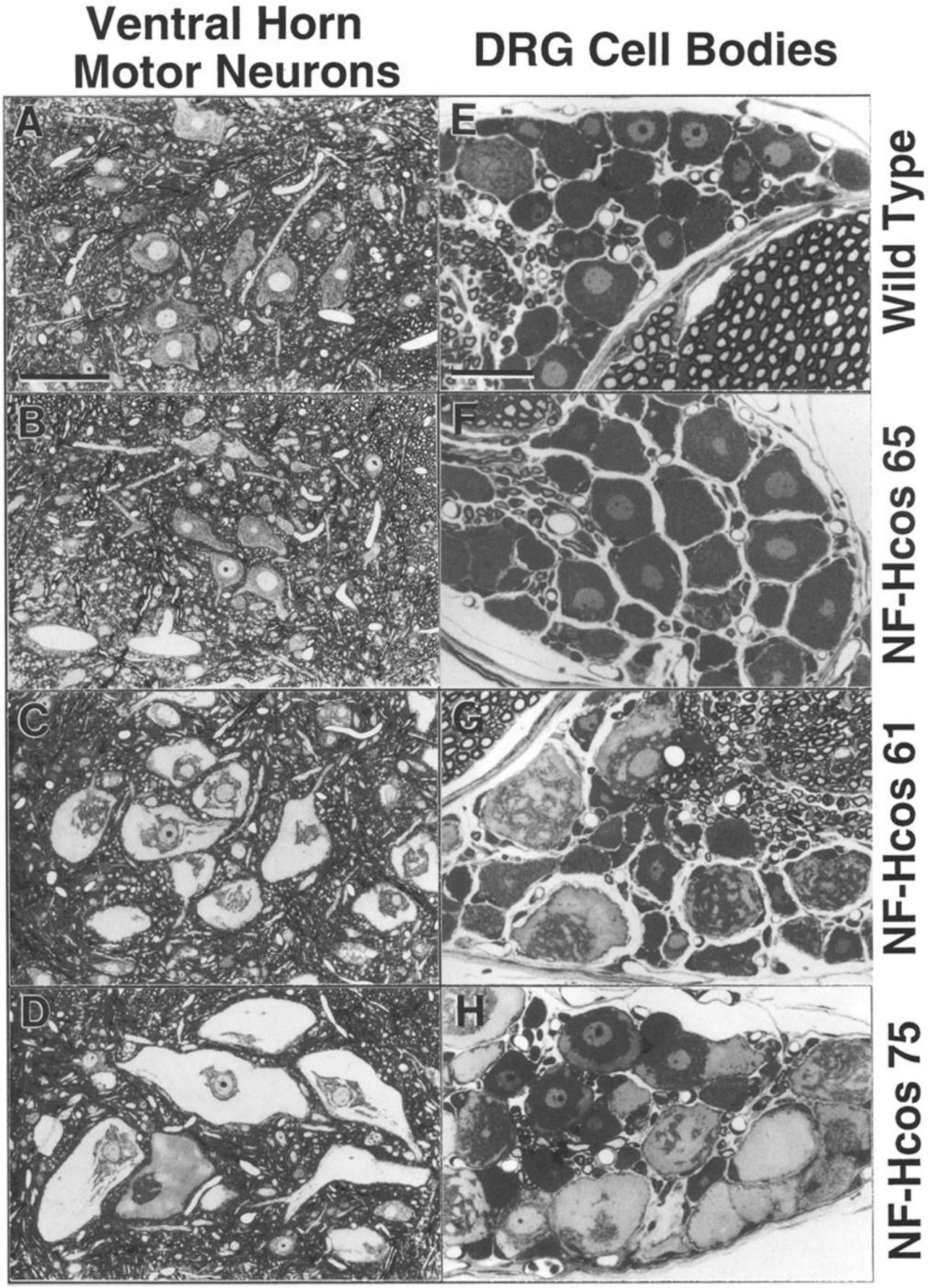
Ventral Horn
Motor Neurons
DRG Cell Bodies
A
B
C
D
E
F
G
H
Wild Type
NF-Hcos 65
NF-Hcos 61
NF-Hcos 75

To test directly if increase in NF-H synthesis affects the rate of neurofilament transport into and along the axon in a dosage-dependent manner, axonal transport rates of neurofilaments were initially examined in motor neurons of nontransgenic mice and mice expressing the highest level of NF-H (line NF-Hcos 75). The distribution of radiolabeled polypeptides in both the soluble and cytoskeletal phases in the ventral root and the sciatic nerve, representing the transport of newly synthesized neurofilament subunits into and along the motor axons, was determined at 14 d after the injection of [^{35}S]methionine into the ventral horn of the spinal cord (Fig. 8). In the transgenic mice expressing increased levels of NF-H, transported NF-H and NF-L were primarily in the insoluble fraction, as was also the case for nontransgenic animals, but the rate of transport was markedly retarded. In the normal mouse, a peak of radioactivity for NF-L, NF-M, and NF-H was found at segment 2, a distance ~8 mm from the cell bodies, corresponding to a transport rate of 0.6 mm/d. In the NF-H transgenic mice, neurofilament transport was decreased both in amount and in speed (by 2 wk after injection, the peak had not yet entered the segments available for analysis, indicating a slowing by at least two- to threefold). This was a selective retardation of neurofilament subunits, as transport of other components in the insoluble phase was unaltered. Moreover, increased synthesis of NF-H resulted in a selective (approximately twofold) reduction (compared with NF-L) in the amount of NF-M transported (e.g., see cytoskeletal phases of Fig. 8, *A* and *B*), consistent with the lower axonal content of NF-M (Fig. 3 *B*) and the lower level of NF-M mRNA in the spinal cords (Fig. 2 *A*). Inspection of the soluble phase revealed that the amount other cargoes moved in slow axonal transport, such as tubulin and actin (and an unidentified protein marked with an asterisk in Fig. 8), was undiminished, while the velocity was modestly elevated (especially apparent for tubulin, Fig. 8 *B*, *right*). Thus, in motor axons, increased synthesis of NF-H leads to selective reduction in the amount and rate of transport of neurofilament subunits, while transport of other components of slow transport are accelerated in transit rate.

Axonal transport rates of neurofilaments were also examined in sensory axons from normal mice or from mice expressing a modest increase in NF-H synthesis (line NF-Hcos 65) and high levels of NF-H synthesis (line NF-Hcos 61). Transport of neurofilament subunit-associated radioactivity in each of the 3-mm segments was quantified by phosphorimaging. To standardize comparison among multiple animals, the signals were converted to percentage of total radioactivity and are displayed in Fig. 9, *D–I*. In the nontransgenic mice, the peak of newly synthesized neurofilaments moved along the axon at ~1-1.2 mm/d, a value in agreement with the expected rate of neurofilament transport in sensory axons (Hoffman and Lasek, 1975; Hoffman et al., 1983). In line NF-Hcos65, the increase in NF-H content slowed neurofilament transport slightly (to ~0.8–0.9 mm/d). A larger increase (~3.5-fold) in NF-H expression (NF-Hcos 61) retarded neurofilament transport to <50% of the nontransgenic rate. In addition, an increased level of NF-H also correlated with a selective loss of NF-M subunits in the axonally transported subunits (compare Fig. 9, *A* and 9 *C*), in agreement with the reduction in accumulated axonal NF-M (Fig. 3 *B*).

Increase in Mouse NF-H Expression Does Not Result in Disease or Motor Neuron Degeneration or Death

In transgenic mice expressing wild-type human NF-H mRNA at twofold over the endogenous murine NF-H mRNA levels, perikaryal and axonal accumulations of neurofilaments in neurons, slowing of axonal neurofilament transport, and reduction in caliber of large myelinated motor axons have been reported to be accompanied by development of overt clinical abnormalities beginning at as early as 3–4 mo of age and characterized by fine tremors, fore-limb weakness, and neurogenic muscle atrophy (Cote et al., 1993; Collard et al., 1995). Although the extent of increase in NF-H expression, the cytoskeletal abnormalities, and decrease in axonal neurofilament transport observed in the murine NF-H transgenic mice are similar to that of the human NF-H transgenic mice, none of the five murine NF-H transgenic lines develop an obvious phenotype, even at >2 yr of age. Rather, kinetic activity, weight gain, muscle mass, and life span are indistinguishable from nontransgenic littermates.

To determine if there are presymptomatic changes that are consistent with development of motor neuron disease, the three highest expressing lines (35, 61, and 75) were examined at up to 2 yr of age for any significant loss of motor neurons and for development of muscle atrophy. In contrast to the human NF-H transgenic mice, detailed microscopic examination of sections from multiple skeletal muscles failed to show any signs of neurogenic atrophy of the muscle fibers in any of the lines of murine NF-H transgenic mice. Even very aged (2-yr-old) animals of the highest expressing line (line 75) revealed no statistically significant loss in motor neurons (as determined by counting the number of surviving axons in the L4 and L5 ventral roots; Fig. 10 *C*) and no muscle atrophy (Fig. 10 *A*), despite chronically decreased axonal caliber and continuous perikaryal accumulations in motor neurons (Fig. 10 *A*) that resulted in much more grossly distended cell bodies than those seen in mice developing disease from increased expression of murine NF-L (Xu et al., 1993) or human NF-H (Cote et al., 1993). Prominent proximal swellings in motor neuron axons were seen at all ages. For example, Fig. 10 *B* displays an axonal spheroid (*arrow*) appearing in the proximal-most myelinated portion of an axon emerging from a motor neuron cell body containing masses of lightly stained neurofilaments from a 2-yr-old NF-H line 75 mouse. However, these swellings were less frequent than in the NF-L (Xu et al., 1993) transgenic animals, and in the NF-H mice, not only was there an absence of neuronal loss, but other markers frequently found in neurodegenerative disease

Figure 4. Neurofilamentous accumulation in cell bodies of ventral horn motor neurons in NF-H transgenic mice. Light micrographs of 1-μm plastic sections (stained with toluidine blue) of (*A–D*) ventral horn motor neurons at the lumbar bulge and (*E–H*) L5 dorsal root ganglion cell bodies in wild-type and transgenic lines NF-Hcos-65, NF-Hcos-61, and NF-Hcos-75. Bars, 100 μm.

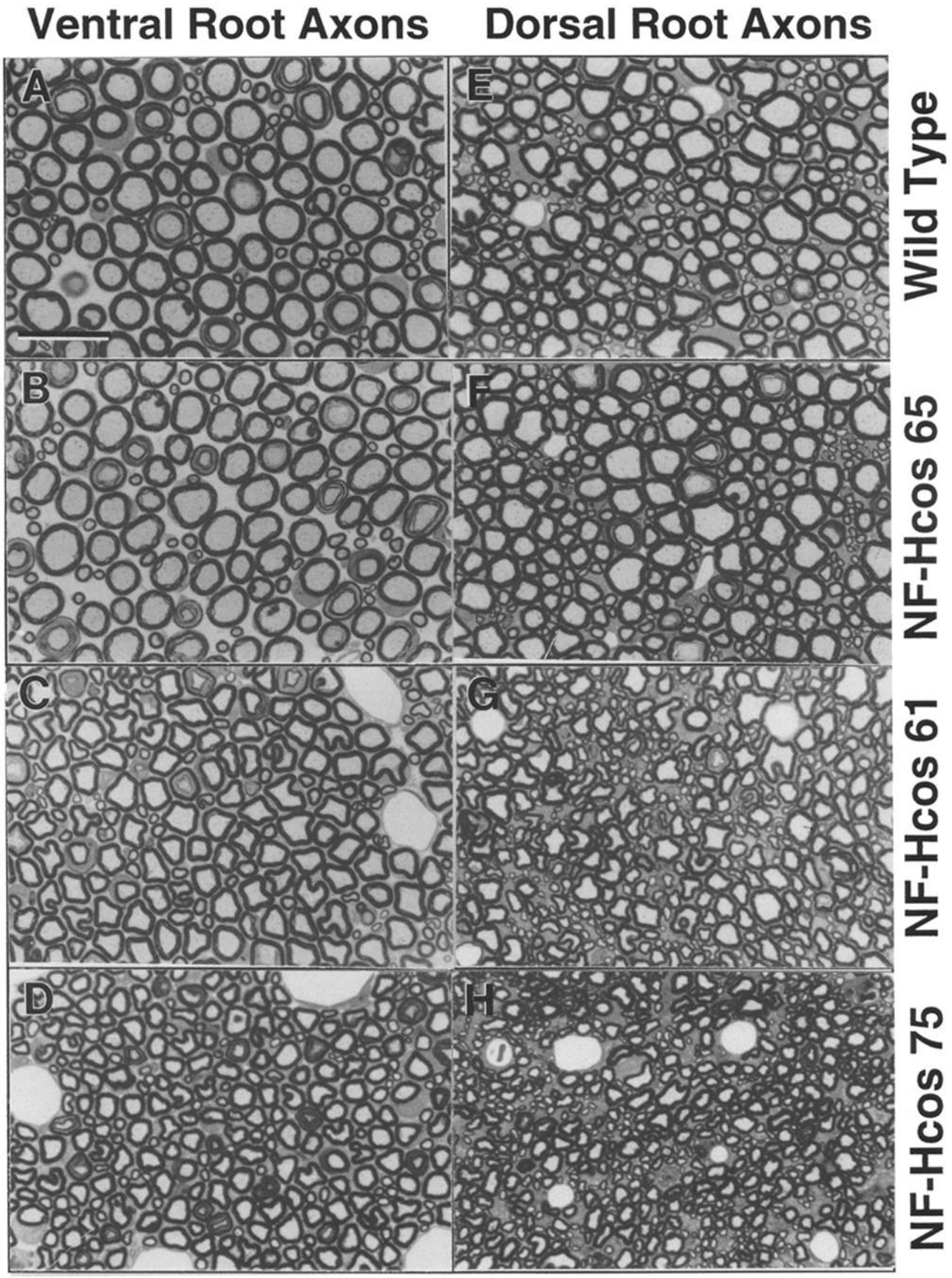

Figure 5. Calibers of motor (ventral root) and sensory (dorsal root) neurons in NF-H transgenic mice. (*A–D*) Ventral root axons. (*E–H*) Dorsal root axons. Bar, 20 μm.

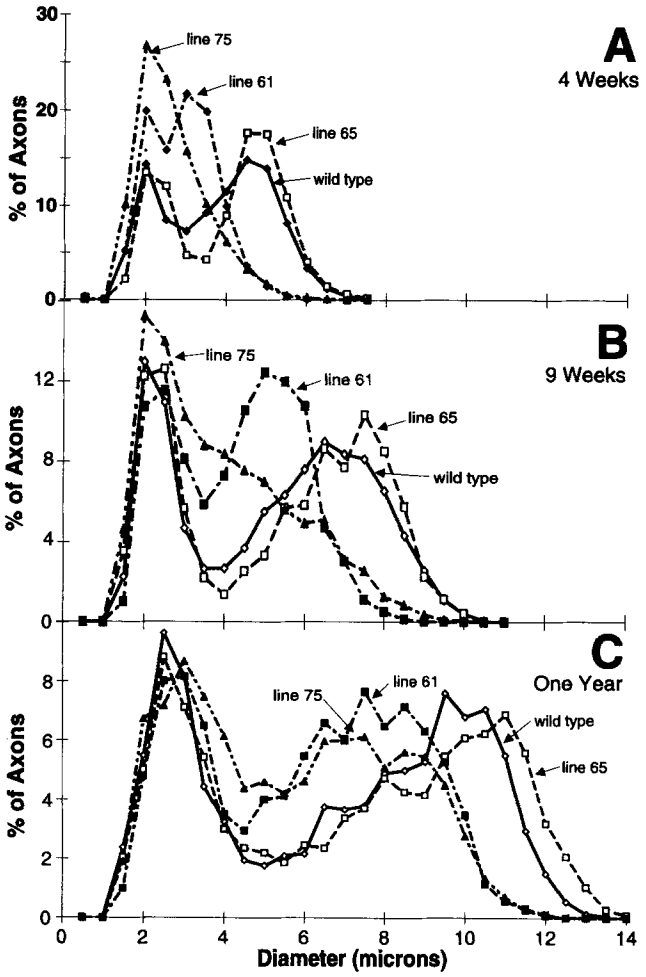

Figure 6. NF-H dosage-dependent changes in axonal caliber in ventral root axons. (*A*) Distribution of diameters of axons in the L5 ventral root of (*A*) 4-wk-, (*B*) 9-wk-, or (*C*) 1-yr-old animals.

were also absent. For example, there was no reactive astrocytosis, as judged by immunocytochemistry with antibodies to glial fibrillary acid protein (data not shown). Nor did there appear to be loss of mitochondria in axons from the NF-H mice; instead, morphologically normal mitochondria were found in the transgenic axons at the same frequency per axonal cross-sectional area as the present in wild-type axons (e.g., see Fig. 10 *A*).

Like the situation in lower motor and sensory neurons, an initial survey of the brains of line 75 mice revealed that the increased synthesis of NF-H led to neurofilamentous swellings in the perikarya and proximal axons in many neurons, most prominently in the brain stem. Many of these also displayed signs of vacuolar degeneration, and there was extracellular mineral deposition in affected regions, indicating that the increased burden of NF-H does cause subclinical affects in some central nervous system neurons. The remainder of the cortical, subcortical, and cerebellar neuronal populations appeared normal.

Discussion

Earlier indirect evidence implicated a primary role for NF-H in determination and maintenance of axonal caliber and as

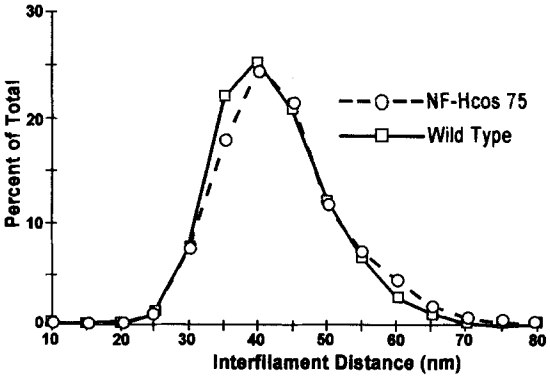

Figure 7. Distribution of nearest neighbor distances between neurofilaments in ventral root axons from (○) NF-Hcos 75 transgenic mice or (□) nontransgenic littermate control mice.

a rate-determining factor in slow axonal transport. The present analysis of transgenic mice that express wild-type murine NF-H to varying levels demonstrates that changes in NF-H synthesis and accumulation can mediate both of these events. By varying NF-H levels, two seemingly different effects occur: mild enhancement of radial growth of large myelinated axons by modest increases in NF-H (and total NF subunit) levels (Figs. 3 and 5), but inhibition of radial growth concomitant with greater overexpression and decrease in axonal neurofilaments. It seems likely that

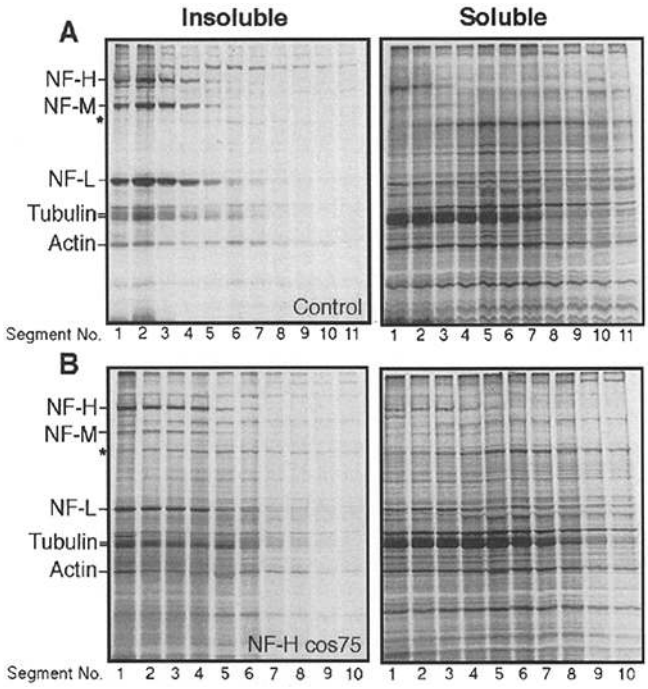

Figure 8. Increasing NF-H levels causes selective slowing of neurofilament transport in motor axons. Transport of radiolabeled proteins in motor axons of the sciatic nerve from a (*A*) 8-wk-old nontransgenic mouse and (*B*) an age-matched NF-Hcos 75 mouse. Fluorographs representing successive 3-mm segments from the sciatic nerve are shown both for cytoskeletal (insoluble) fractions as well as for the soluble component of transport. The asterisk marks the mobility of a ~120-kD transported polypeptide present in both soluble and insoluble compartments.

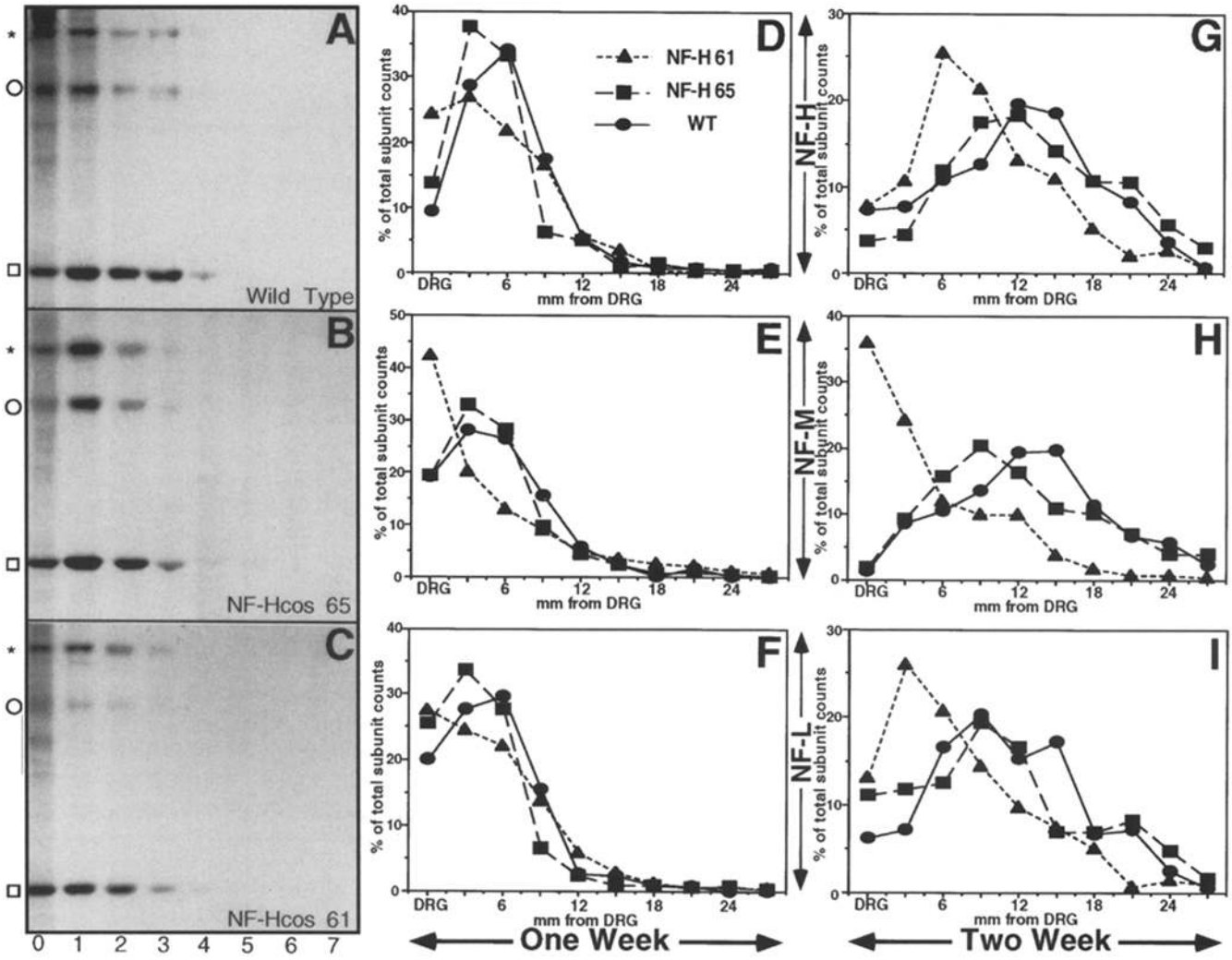

Figure 9. NF-H–dependent slowing of axonal transport in sensory neurons. Fluorographs of neurofilament protein transport after injection of [^{35}S]methionine into dorsal root ganglia. Each lane represents a 3-mm distal segment from the sciatic nerve of 7-wk-old animals killed 7 d after injection. (*A*) Wild type. (*B*) NF-Hcos 65. (*C*) NF-Hcos 61. Transport of neurofilament subunits quantified by phosphorimaging at (*D–F*) 7 and (*G–I*) 14 d after labeling. Each value represents the average of three animals.

the two effects result from the same mechanism: increased abundance of NF-H (Figs. 2 *B* and 3 *B*) decreases the rate of neurofilament transport (Figs. 8 and 9) without affecting the content of other structural components (e.g., tubulin; Fig. 3 *A*). With production of a constant overall level of newly synthesized subunits (the sum of NF-L, NF-M, and NF-H) in perikarya, a small increase in the proportion of NF-H (Fig. 3, for lines 62 and 65) slows transport (Fig. 8) and yields increased neurofilaments in proximal axons (Fig. 3 *B*), thereby producing larger axons with no perikaryal abnormalities. However, if transport is slowed further, production of neurofilaments exceeds the rate at which they enter axons, causing neurofilamentous accumulations in the cell bodies. A secondary consequence of retention of neurofilaments in the cell body is reduction of neurofilament content in axons (Fig. 3 *B*) and a consequent inhibition of radial growth of large myelinated axons.

Concerning the mechanism of neurofilament-mediated radial growth, in combination with earlier transgenic mice expressing elevated levels of murine NF-L (Monteiro et al., 1990; Xu et al., 1993) and epitope-tagged NF-M (Wong et al., 1995*a*), it is now clear that significant increases in any single neurofilament subunit inhibit growth in caliber. On the other hand, modest increases in both NF-L and either NF-M or NF-H significantly promote radial growth (Xu et al., 1996). As proposed earlier (Xu et al., 1996), the simplest view is that radial growth requires all three subunits: NF-L to support filament assembly, and a scaffolding of NF-M

Figure 10. Pathologic consequences of continuous overexpression of wild-type murine NF-H in 2-yr-old animals. (*A*) Ventral horn motor neurons and skeletal muscle. (*B*) Proximal axonal swellings in ventral horn of spinal cord in a 2-yr-old NF-Hcos 75 mouse. (*Arrow*) Proximal axonal swelling. (*Arrowheads*) Unmyelinated initial axonal segment. (*C*) Total number of axons in the L4 and L5 ventral roots of 2-yr-old wild-type NF-Hcos 75 mice. (n = 3 for wild-type; n = 2 for NF-Hcos 75.) Bars: (*A*) 100 μm (*top*), 20 μm (*middle*), 100 μm (*bottom*); (*B*) 50 μm.

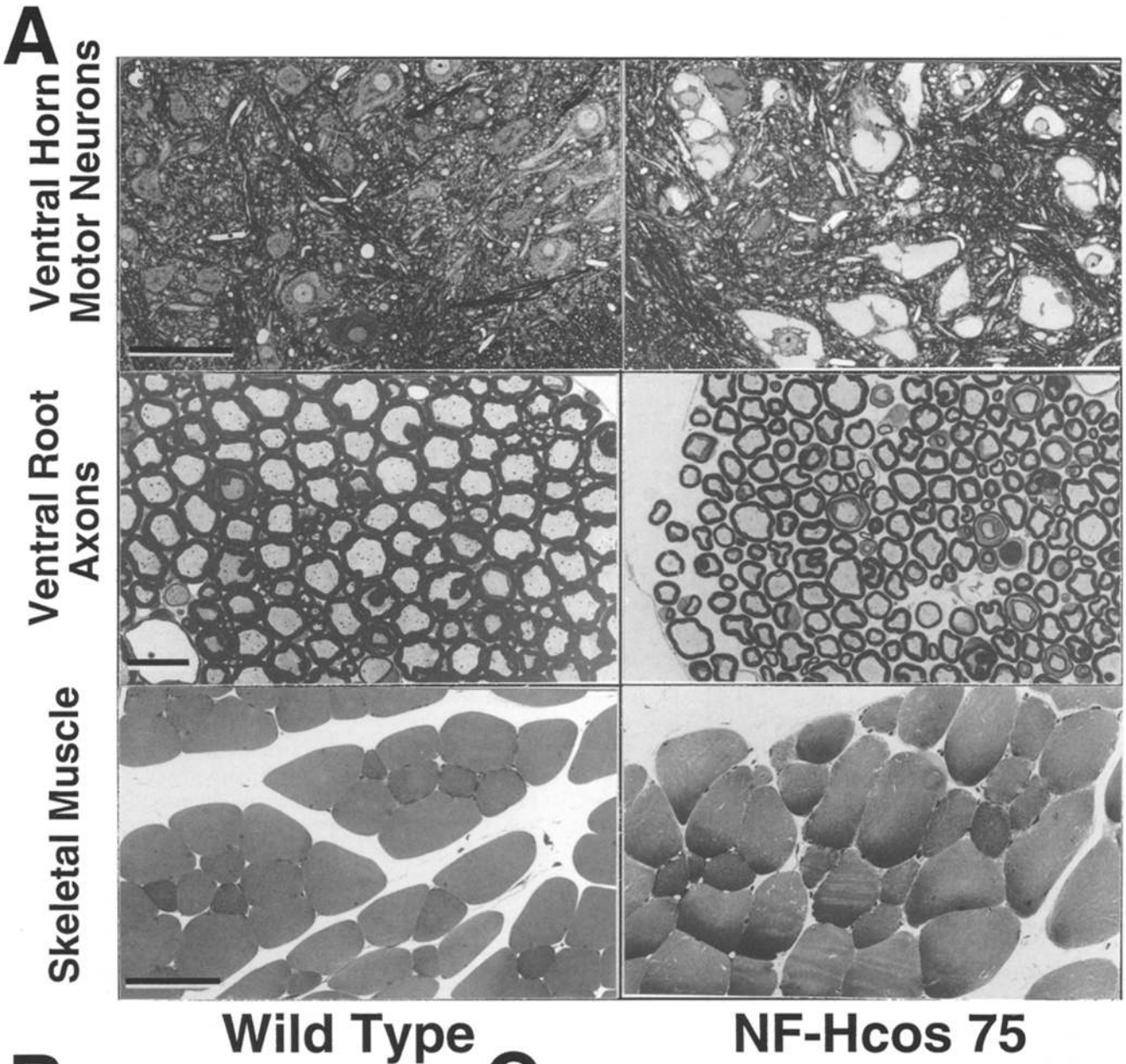
A
Ventral Horn Motor Neurons
Ventral Root Axons
Skeletal Muscle
Wild Type
NF-Hcos 75

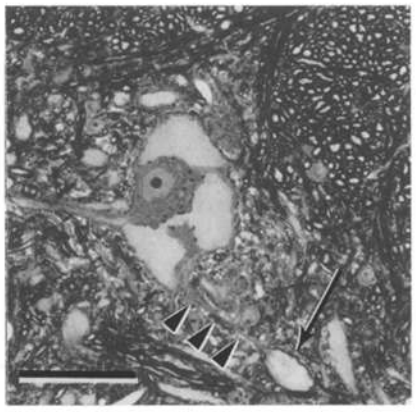
B

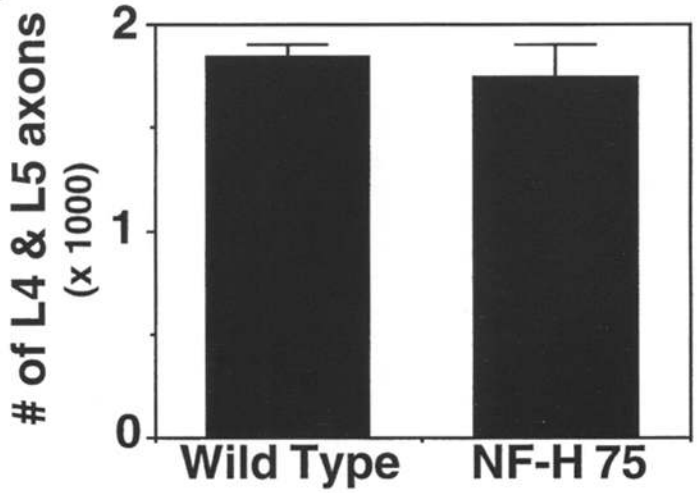
C
# of L4 & L5 axons
(x 1000)
2
1
0
Wild Type
NF-H 75

and NF-H tails crossbridged between neurofilaments and/or other axonal components. What is clear, however, is that changing the content of NF-H (with a corresponding reduction in NF-M) does not affect nearest neighbor spacing of neurofilaments, a finding that goes hand in hand with the identical situation after doubling axonal NF-M and a corresponding loss in NF-H (Wong et al., 1995*a*). Since radial growth can be markedly inhibited despite no change in interfilament distance, this finding gives additional weight to the argument that interactions between nearest neighbor filaments do not specify radial growth. The key property(ies) needed to stimulate caliber growth must include longer range interactions between neurofilaments that are not nearest neighbors or between neurofilaments and other axonal components. Attractive candidates for these additional interactions include the family of proteins such as BPAG1n, proven recently to crossbridge between neurofilaments and actin filaments in sensory neurons (Yang et al., 1996).

One probable mechanism through which elevated synthesis of NF-H retards neurofilament transport is by shifting an equilibrium toward assembly of stationary neurofilaments. Two pools of neurofilaments (and/or neurofilament subunits) are known in axons, one moving at the traditionally measured slow axonal transport rate and the other essentially stationary (Nixon and Logvinenko, 1986; Lasek et al., 1992), although there is disagreement over the magnitude of the stationary phase. Assuming that subunits reversibly cycle from the stationary phase back to the moving phase, an obvious possibility would be that NF-H tail-dependent crossbridging between filaments and/or to other axonal components yields a shift to the immobile (or less mobile) phase in the axons. In the cell bodies, similar cross-linking may block access of oligomers and/or polymers as initial substrates for entering the transport machinery, hence resulting in perikarya swollen with assembled neurofilaments.

Lastly, the absence of disease, motor neuron death, or denervation atrophy of skeletal muscle even in aged animals expressing wild-type mouse NF-H at up to 4.5 times its normal rate offers strong evidence for the view that motor neurons are remarkably tolerant of misaccumulated neurofilaments assembled from wild-type subunits. No significant death of motor neurons is found in aged animals despite perikarya chronically distended with large masses of filaments, massive proximal axonal swellings (Fig. 10 *B*), and distal axonal atrophy (Figs. 5 *D* and 10 *A*). This contrasts sharply with the situation arising from expressing two to three times lower levels of human NF-H (Cote et al., 1993). The human NF-H subunit, which differs from mouse NF-H in >160 amino acid positions scattered throughout the polypeptide backbone (counting the many sequence differences in the long KSP repeat domain as only a single difference; Julien et al., 1988; Lees et al., 1988), results in progressive neuronopathy (Cote et al., 1993), inhibition of radial growth, and increased frequency of axonal degeneration (Collard et al., 1995), albeit without significant decrease in axon number even in aged animals (e.g., see total wild-type and transgenic axon number in Fig. 1 *b* of Collard et al., 1995).

Disease developed by animals accumulating human NF-H led to the initial proposal that modest upregulation of NF-H cross-linkers impairs neurofilament transport, causing neuronal swellings with ensuing axonopathy and muscle atrophy (Cote et al., 1993; Collard et al., 1995). However, the absence of disease in any mice expressing varying amounts of mouse NF-H shows that the wild-type NF-H cannot provoke similar disease, despite slowing of neurofilament transport to a comparable extent. The combined data instead strongly support the view that human NF-H causes disease in mice by acting as an aberrant, mutant subunit. A similar situation has already emerged from analysis of mice expressing wild-type or mutant NF-L subunits. A doubling of murine NF-L content (and a corresponding increase in axonal neurofilaments) does not result in disease (Monteiro et al., 1990; Xu et al., 1993), whereas accumulation of one fourth as much of a point mutant in NF-L reproduces most features of ALS, including selective death of motor neurons (Lee et al., 1994). Wild-type NF-L produces disease only when expressed at a level that yields four times the normal number of axonal neurofilaments (Xu et al., 1993), ten times more than required to produce disease from accumulation of the mutant NF-L subunit, and even at this level, the wild-type protein does not cause motor neuron death. That neurons are remarkably tolerant of wild-type neurofilaments is also consistent with the massive intraaxonal accumulation of NFs resulting from selective detachment of neurofilaments from slow transport after administration of the drug β,β′-iminodiproprionitrile (IDPN). The giant axonal swellings do not yield neuronal death and disappear when IDPN is withdrawn (Clark et al., 1980).

The combined findings offer strong support for the view that neurofilament-dependent dysfunction, degeneration, and/or death of motor neurons in mice are mediated through disorganized arrays of filaments impeding axonal transport, not only of neurofilaments (as seen in the mice expressing wild-type mouse NF-H presented here) but also of other components in both anterograde and/or retrograde movement (as seen in mice expressing human NF-H; Collard et al., 1995). Further evidence that disorganized neurofilament arrays can be toxic to neurons has emerged from analysis of the absence of the neuronal isoform of BPAG1 (referred to as BPAG1n [Yang et al., 1996] or dystonin [Brown et al., 1995]), a protein normally expressed exclusively in sensory neurons and that cross-links actin filaments and neurofilaments (Yang et al., 1996). In the absence of BPAG1n-dependent cross-linking, axonal architecture is markedly perturbed (Yang et al., 1996), and there is widespread degeneration and death of sensory neurons (Brown et al., 1995; Guo et al., 1995).

Relative to the pathogenesis of disease, damage to and disorganization of filaments could arise either from direct mutation in neurofilaments (as proven in mice; Lee et al., 1994), from any number of posttranslational events, or from mutation in neurofilament-associated components (e.g., BPAG1n; Yang et al., 1996). Consistent with the first of these findings, in sporadic human ALS, two deletions in the KSP repeat domain of NF-H have been identified in five of 356 patients (Figlewicz et al., 1994). It must be admitted, however, that examination of the KSP repeat domain of NF-H (Rooke et al., 1996) or the entirety of the coding domains of NF-L, NF-M, or NF-H (Vechio et al., 1996) have failed to uncover mutations linked to disease in

>100 familial ALS DNAs examined thus far, so it seems unlikely that neurofilament mutations can account for a significant proportion (if any) of inherited ALS. On the other hand, in the 20% of familial ALS caused by mutation in the enzyme superoxide dismutase 1 (Rosen et al., 1993), disease (at least in mice) arises from a toxic property of the mutant subunit (Wong et al., 1995*b*). Although the relevant toxic property(ies) is not yet identified, two plausible proposals are mutant enzyme-mediated nitration of protein-bound tyrosines (Beckman et al., 1993) or action of the mutants as peroxidases (Wiedau-Pazos et al., 1996). Neurofilaments, as abundant and long-lived proteins, are attractive candidates for progressively accumulating such chemical damage. Indeed, neurofilament accumulations are hallmarks of sporadic (Hirano et al., 1984*a*) and familial (Hirano et al., 1984*b*) disease, and they are especially conspicuous in disease mediated by superoxide dismutase mutations (e.g., for mutations A4V [Hirano et al., 1984*a*]; Shibata et al., 1996; and I113T [Rouleau et al., 1996]). In conjunction with the earlier evidence from Julien and colleagues (Cote et al., 1993; Collard et al., 1995), the sum of the evidence thus strongly supports the view that aberrant accumulations of axonal neurofilaments, whether primary or seconday insults, mediate neuronal failure through strangulation of the axonal transport that is so crucial to these large asymmetric cells.

We thank J.-P. Julien for generously providing a cosmid containing the mouse NF-H gene, V. Lee for providing antibodies to NF-H, and N. Jenkins of Frederick Cancer Center for initial production of transgenic mice. We also thank Ms. Janet Folmer and Ms. Karen Anderson for their expert assistance with microscopy.

This work has been supported by grant NS27036 from the National Institutes of Health (NIH) to D.W. Cleveland. D.W. Cleveland is the recipient of an NIH Jacob Javits Neuroscience Investigator award. M.K. Lee and Z. Xu were supported in part by postdoctoral fellowships from the NIH and the Muscular Dystrophy Association, respectively.

Received for publication 18 April 1996 and in revised form 31 July 1996.

References

Arbuthnott, E.R., I.A. Boyd, and K.U. Kalu. 1980. Ultrastructural dimensions of myelinated peripheral nerve fibres in the cat and their relation to conduction velocity. *J. Physiol.* 308:125–137.

Beckman, J.S., M. Carson, C.D. Smith, and W.H. Koppenol. 1993. ALS, SOD and peroxynitrite. *Nature (Lond.).* 364:584.

Brown, A., G. Bernier, M. Mathieu, J. Rossant, and R. Kothary. 1995. The mouse dystonia musculorum gene is a neural isoform of bullous pemphigoid antigen 1. *Nat. Genet.* 10:301–306.

Carpenter, S. 1968. Proximal axonal enlargement in motor neuron disease. *Neurology.* 18:841–851.

Ching, G.Y., and R.K. Liem. 1993. Assembly of type IV neuronal intermediate filaments in nonneuronal cells in the absence of preexisting cytoplasmic intermediate filaments. *J. Cell Biol.* 122:1323–1335.

Chou, S.M., and A.V. Fakadej. 1971. Ultrastructure of chromatolytic motor neurons and anterior spinal roots in a case of Werdnig-Hoffman disease. *J. Neuropathol. Exp. Neurol.* 30:42–55.

Clark, A.W., J.W. Griffin, and D.L. Price. 1980. The axonal pathology in chronic IDPN intoxication. *J. Neuropathol. Exp. Neurol.* 39:42–55.

Cleveland, D.W., M.J. Monteiro, P.C. Wong, S.R. Gill, J.D. Gearhart, and P.N. Hoffman. 1991. Involvement of neurofilaments in the radial growth of axons. *J. Cell Sci. Suppl.* 15:85–95.

Collard, J.F., F. Cote, and J.P. Julien. 1995. Defective axonal transport in a transgenic mouse model of amyotrophic lateral sclerosis. *Nature (Lond.).* 375:61–64.

Cote, F., J.F. Collard, and J.P. Julien. 1993. Progressive neuronopathy in transgenic mice expressing the human neurofilament heavy gene: a mouse model of amyotrophic lateral sclerosis. *Cell.* 73:35–46.

de Waegh, S.M., V.M. Lee, and S.T. Brady. 1992. Local modulation of neurofilament phosphorylation, axonal caliber, and slow axonal transport by myelinating Schwann cells. *Cell.* 68:451–463.

Eyer, J., and A. Peterson. 1994. Neurofilament-deficient axons and perikaryal aggregates in viable transgenic mice expressing a neurofilament-β-galactosidase fusion protein. *Neuron.* 12:389–405.

Figlewicz, D.A., A. Krizus, M.G. Martinoli, V. Meininger, M. Dib, G.A. Rouleau, and J.-P. Julien. 1994. Variants of the heavy neurofilament subunit are associated with the development of amyotrophic lateral sclerosis. *Hum. Mol. Genet.* 3:1757–1761.

Friede, R.L., and T. Samorajski. 1970. Axon caliber related to neurofilaments and microtubules in sciatic nerve fibers of rats and mice. *Anat. Rec.* 167:379–387.

Gasser, H.S., and H. Grundfest. 1939. Axon diameters in relation to the spike dimensions and the conduction velocity in mammalian A fibers. *Am. J. Physiol.* 127:393–414.

Guo, L., L. Degenstein, J. Dowling, Q.C. Yu, R. Wollmann, B. Perman, and E. Fuchs. 1995. Gene targeting of BPAG1: abnormalities in mechanical strength and cell migration in stratified epithelia and neurologic degeneration. *Cell.* 81:233–243.

Hirano, A. 1991. Cytopathology of amyotrophic lateral sclerosis. *In* Advances in Neurology. Volume 56. Amyotrophic Lateral Sclerosis and Other Motor Neuron Diseases. L.P. Rowland, editor. Raven Press, New York. 91–101.

Hirano, A., H. Donnenfeld, S. Sasaki, and I. Nakano. 1984*a*. Fine structural observations of neurofilamentous changes in amyotrophic lateral sclerosis. *J. Neuropathol. Exp. Neurol.* 43:461–470.

Hirano, A., I. Nakano, L.T. Kurland, D.W. Mulder, P.W. Holley, and G. Saccomanno. 1984*b*. Fine structural study of neurofibrillary changes in a family with amyotrophic lateral sclerosis. *J. Neuropathol. Exp. Neurol.* 43:471–480.

Hirokawa, N., M.A. Glicksman, and M.B. Willard. 1984. Organization of mammalian neurofilament polypeptides within the neuronal cytoskeleton. *J. Cell Biol.* 98:1523–1536.

Hoffman, P.N., and R.J. Lasek. 1975. The slow component of axonal transport. Identification of major structural polypeptides of the axon and their generality among mammalian neurons. *J. Cell Biol.* 66:351–366.

Hoffman, P.N., R.J. Lasek, J.W. Griffin, and D.L. Price. 1983. Slowing of the axonal transport of neurofilament proteins during development. *J. Neurosci.* 3:1694–1700.

Hoffman, P.N., J.W. Griffin, and D.L. Price. 1984. Control of axonal caliber by neurofilament transport. *J. Cell Biol.* 99:705–714.

Hoffman, P.N., D.W. Cleveland, J.W. Griffin, P.W. Landes, N.J. Cowan, and D.L. Price. 1987. Neurofilament gene expression: a major determinant of axonal caliber. *Proc. Natl. Acad. Sci. USA.* 84:3472–3476.

Hsieh, S.-T., G.J. Kidd, T.O. Crawford, Z.-S. Xu, B.D. Trapp, D.W. Cleveland, and J.W. Griffin. 1994. Regional modulation of neurofilament organization by myelination in normal axons. *J. Neurosci.* 14:6392–6401.

Julien, J.P., F. Cote, L. Beaudet, M. Sidky, D. Flavell, F. Grosveld, and W. Mushynski. 1988. Sequence and structure of the mouse gene coding for the largest neurofilament subunit. *Gene (Amst.).* 68:307–314.

Lasek, R.J., P. Paggi, and M.J. Katz. 1992. Slow axonal transport mechanisms move neurofilaments relentlessly in mouse optic axons. *J. Cell Biol.* 117: 607–616.

Lee, M.K., and D.W. Cleveland. 1994. Neurofilament function and dysfunction: involvement in axonal growth and neuronal disease. *Curr. Opin. Cell Biol.* 6: 34–40.

Lee, M.K., J.B. Tuttle, L.I. Rebhun, D.W. Cleveland, and A. Frankfurter. 1990. The expression and posttranslational modification of a neuron-specific β-tubulin isotype during chick embryogenesis. *Cell Motil. Cytoskeleton.* 17: 118–132.

Lee, M.K., Z. Xu, P.C. Wong, and D.W. Cleveland. 1993. Neurofilaments are obligate heteropolymers in vivo. *J. Cell Biol.* 122:1337–1350.

Lee, M.K., J.R. Marszalek, and D.W. Cleveland. 1994. A mutant neurofilament subunit causes massive, selective motor neuron death: implications for the pathogenesis of human motor neuron disease. *Neuron.* 13:975–988.

Lee, V.M., M.J. Carden, W.W. Schlaepfer, and J.Q. Trojanowski. 1987. Monoclonal antibodies distinguish several differentially phosphorylated states of the two largest rat neurofilament subunits (NF-H and NF-M) and demonstrate their existence in the normal nervous system of adult rats. *J. Neurosci.* 7:3474–3488.

Lees, J.F., P.S. Shneidman, S.F. Skuntz, M.J. Carden, and R.A. Lazzarini. 1988. The structure and organization of the human heavy neurofilament subunit (NF-H) and the gene encoding it. *EMBO (Eur. Mol. Biol. Organ.) J.* 7:1947–1955.

Lopata, M.A., and D.W. Cleveland. 1987. In vivo microtubules are copolymers of available beta-tubulin isotypes: localization of each of six vertebrate beta-tubulin isotypes using polyclonal antibodies elicited by synthetic peptide antigens. *J. Cell Biol.* 105:1707–1720.

Monteiro, M.J., P.N. Hoffman, J.D. Gearhart, and D.W. Cleveland. 1990. Expression of NF-L in both neuronal and nonneuronal cells of transgenic mice: increased neurofilament density in axons without affecting caliber. *J. Cell Biol.* 111:1543–1557.

Nixon, R.A., and K.B. Logvinenko. 1986. Multiple fates of newly synthesized neurofilament proteins: evidence for a stationary neurofilament network distributed nonuniformly along axons of retinal ganglion cell neurons. *J. Cell Biol.* 102:647–659.

Nixon, R.A., P.A. Paskevich, R.K. Sihag, and C.Y. Thayer. 1994. Phosphorylation on carboxyl terminus domains of neurofilament proteins in retinal ganglion cell neurons in vivo: influences on regional neurofilament accumulation, interneurofilament spacing, and axon caliber. *J. Cell Biol.* 126:1031–1046.

Ohara, O., Y. Gahara, T. Miyake, H. Teraoka, and T. Kitamura. 1993. Neurofilament deficiency in quail caused by nonsense mutation in neurofilament-L gene. *J. Cell Biol.* 121:387–395.

Rooke, K., D.A. Figlewicz, F. Han, and G.A. Rouleau. 1996. Analysis of the KSP repeat of the neurofilament heavy subunit in familial amyotrophic lateral sclerosis. *Ann. Neurol.* 46:789–790.

Rosen, D.R., T. Siddique, D. Patterson, D.A. Figlewicz, P. Sapp, A. Hentati, D. Donaldson, J. Goto, J.P. O'Regan, H.X. Deng et al. 1993. Mutations in Cu/Zn superoxide dismutase gene are associated with familial amyotropic lateral sclerosis. *Nature (Lond.).* 362:59–62.

Rouleau, G.A., A.W. Clark, K. Rooke, A. Pramatarova, A. Krizus, O. Suchowersky, J.-P. Julien, and D. Figlewicz. 1996. SOD1 mutation is associated with accumulation of neurofilaments in amyotrophic lateral scleorsis. *Ann. Neurol.* 39:128–131.

Sakaguchi, T., M. Okada, T. Kitamura, and K. Kawasaki. 1993. Reduced diameter and conduction velocity of myelinated fibers in the sciatic nerve of a neurofilament-deficient mutant quail. *Neurosci. Lett.* 153:65–68.

Schlaepfer, W.W., and J. Bruce. 1990. Neurofilament proteins are distributed in a diminishing proximodistal gradient along rat sciatic nerve. *J. Neurochem.* 55:453–460.

Shibata, N., A. Hirano, M. Kobayashi. T. Siddique, H.-X. Deng, W.-Y. Hung, T. Kato, and K. Asayama. 1996. Intense superoxide dismutase-1 immunoreactivity in intracytoplasmic hyaline inclusions of familial amyotrophic lateral sclerosis with posterior column involvement. *J. Neuropathol. Exp. Neurol.* 55:481–490.

Troncoso, J.C., J.L. March, M. Haner, and U. Aebi. 1990. Effect of aluminum and other multivalent cations on neurofilaments in vitro: an electron microscopic study. *J. Struct. Biol.* 103:2–12.

Vechio, J.V., L.I. Bruijn, Z.-S. Xu, R.H. Brown, Jr., and D.W. Cleveland. 1996. Identification of variants in human neurofilament genes: absence of linkage to familial ALS. *Ann. Neurol.* In press.

Wiedau-Pazos, M., J.J. Goto, S. Rabizadeh, E.D. Gralla, J.A. Roe, J.S. Valentine, and D.E. Bredesen. 1996. Altered reactivity of superoxide dismutase in familial amyotrophic lateral sclerosis. *Science (Wash. DC).* 271:515–518.

Willard, M., and C. Simon. 1983. Modulations of neurofilament axonal transport during the development of rabbit retinal ganglion cells. *Cell.* 35:551–559.

Wong, P.C., J. Marszalek, T.O. Crawford, Z. Xu, S.-T. Hsieh, J.W. Griffin, and D.W. Cleveland. 1995*a*. Increasing neurofilament subunit NF-M expression reduces axonal NF-H, inhibits radial growth, and results in neurofilamentous accumulation in motor neurons. *J. Cell Biol.* 130:1413–1422.

Wong, P.C., C.A. Pardo, D.R. Borchelt, M.K. Lee, N.G. Copeland, N.A. Jenkins, S.S. Sisodia, D.W. Cleveland, and D.L. Price. 1995*b*. An adverse property of a familial ALS-linked SOD1 mutation causes motor neuron disease characterized by vacuolar degeneration of mitochondria. *Neuron.* 14:1105–1116.

Xu, Z., L.C. Cork, J.W. Griffin, and D.W. Cleveland. 1993. Increased expression of neurofilament subunit NF-L produces morphological alterations that resemble the pathology of human motor neuron disease. *Cell.* 73:23–33.

Xu, Z.-S., J.R. Marszalek, M.K. Lee, P.C. Wong, J. Folmer, T.O. Crawford, S.-T. Hsieh, J.W. Griffin, and D.W. Cleveland. 1996. Subunit composition of neurofilaments specifies axonal diameter. *J. Cell Biol.* 133:1061–1069.

Yamasaki, H., G.S. Bennett, C. Itakura, and M. Mizutani. 1992. Defective expression of neurofilament protein subunits in hereditary hypotrophic axonopathy of quail. *Lab. Invest.* 66:734–743.

Yang, Y., J. Dowling, Q.-C. Yu, P. Kouklis, D.W. Cleveland, and E. Fuchs. 1996. An essential cytoskeletal linker protein connecting actin microfilaments to intermediate filaments. *Cell.* 86:655–665.